2′-*O*-Methyl-RNA Hairpins Generate Loop−Loop Complexes and Selectively Inhibit HIV-1 Tat-Mediated Transcription†

Fabien Darfeuille,‡ Andrey Arzumanov,§ Michael J. Gait,§ Carmelo Di Primo,‡ and Jean-Jacques Toulmé*,‡

INSERM U386, Université Victor Segalen, 33076 Bordeaux cédex, France, Institut Européen de Chimie et Biologie, 16 avenue Pey Berland, 33607 Pessac, France, and Medical Research Council, Laboratory of Molecular Biology, Hills Road, Cambridge CB2 2QH, U.K.

Received April 16, 2002; Revised Manuscript Received July 17, 2002

ABSTRACT: The interaction of the TAR RNA element of human immunodeficiency virus type 1 (HIV-1) with a 2′-*O*-methyl analogue of an RNA hairpin aptamer previously identified by in vitro selection [Ducongé, F., and Toulmé, J. J. (1999) *RNA 5*, 1605−1614] was characterized by UV-monitored thermal denaturation and surface plasmon resonance experiments. The complex between TAR and this aptamer derivative displays stability ($K_d = 9.9 \pm 1.0$ nM) and kinetic properties [$k_{on} = 9.0 \pm 0.3$ M^{-1} s^{-1}, $k_{off} = (8.9 \pm 0.6) \times 10^{-4}$ s^{-1}] close to those of the parent RNA aptamer. The modified aptamer forms a "kissing" complex with TAR driven by the same key elements as the TAR−RNA aptamer one. In particular, the G and A residues closing the aptamer loop remain crucial for TAR−2′-*O*-methyl aptamer complexes. Moreover, the 2′-*O*-methyl aptamer analogue specifically inhibits Tat-mediated transcription in an in vitro assay more efficiently than the RNA aptamer. This is likely due to the increased lifetime of the former oligonucleotide in the cell-free extract. The 2′-*O*-methyl modification extends the range of molecules that can be used to target viral hairpin RNA through loop−loop interactions. More generally, this demonstrates the interest of SELEX for targeting RNA hairpins and understanding nucleic acid interactions.

Oligonucleotides complementary to an RNA sequence are a powerful means of ablating the expression of any gene of known sequence. The selection of an accessible target region, a crucial step for the success of such an approach, is made difficult as RNAs fold to form secondary and tertiary structures. A number of ways have been explored for the identification of optimal targets (*1*−*3*). Computer-assisted identification of single-stranded regions has been shown to be of limited interest, despite some successful attempts in the design of long antisense sequences (*4*). The shotgun approach, making use of 50−100 individually synthesized oligomers targeted to various regions of an mRNA, is an expansive method which allowed screening on a functional basis (*5*−*7*). Several empirical methods have been reported which correlated target recognition and biological efficacy; this includes RNase H-mediated degradation of RNA portions hybridized to randomly synthesized DNA libraries (*8*), extension of random oligonucleotide pools by reverse transcription (*9*), hybridization to scanning arrays (*10*, *11*), and the use of ribozyme libraries (*12*). These various methods identify accessible sites which generally correspond to single-stranded RNA regions. Consequently, the numerous RNA structures resulting from intramolecular folding are generally not targeted even though a number of them play important roles in gene expression.

Various strategies can be used to generate oligonucleotides that are able to recognize folded RNA structures (*13*). In vitro selection of oligoribonucleotides led to the identification of RNA aptamers against structured RNA from the HCV (*14*) and the HIV-1[1] genomes (*15*, *16*). Hairpin aptamers which form stable kissing complexes with the TAR RNA element of HIV-1 were selected (*15*, *16*). This element, a 59-nucleotide stem−loop structure found at the 5′-untranslated end of all retroviral mRNAs, regulates transcription by interacting with the viral transactivator protein Tat. This protein acts together with host cellular factors, including cyclin T1 and the cyclin-dependent kinase 9 (CDK9), to form a ternary complex at the apical part of TAR. This Tat-associated kinase (TAK) involved in the hyperphosphorylation of the C-terminal domain of RNA polymerase II stimulates the transcriptional efficiency, resulting in an increased level of formation of full-lengh transcripts. Thus, aptamer interference with the upper part of TAR RNA which contains critical protein binding sites would be expected to cripple viral mRNA synthesis and potentially inhibit viral replication.

The use of RNA aptamers in a biological context is of limited interest as these ligands are rapidly degraded by nucleases. The need for chemically modified aptamers has

† F.D. is the recipient of a fellowship from the Agence Nationale de la Recherche sur le SIDA.

* To whom correspondence should be addressed: INSERM U386, Université Victor Segalen, 146 rue Léo Saignat, 33076 Bordeaux cédex, France. Telephone: 33 (0)5 57 57 10 14. Fax: 33 (0)5 57 57 10 15. E-mail: jean-jacques.toulme@bordeaux.inserm.fr.

‡ Université Victor Segalen and Institut Européen de Chimie et Biologie.

§ Medical Research Council.

[1] Abbreviations: CMV, CytoMegaloVirus; HCV, hepatitis C virus; HIV-1, human immunodeficiency virus type 1; OMe, 2′-*O*-methyl oligoribonucleotide; TAR, transactivation responsive element; Tat, transactivator; EMSA, electrophoretic mobility shift assay; SPR, surface plasmon resonance; RU, resonance unit.

10.1021/bi025974d CCC: $22.00
Published on Web 09/13/2002

been previously recognized, and this problem has been addressed in two different ways. On one hand, a few modified nucleotides such as 2′-amino- and 2′-fluoropyrimidine nucleotides (*17*) conferring nuclease resistance are readily incorporated by the enzymes used in the SELEX procedure. On the other hand, chemical modifications can be introduced post-SELEX (*18*). In this case, the positions which can be modified without alteration of the aptamer properties should be carefully identified as chemical modifications may induce conformational changes.

As for anti-TAR kissing aptamers, we considered post-SELEX modifications known to retain the A-type helix geometry adopted by double-stranded RNA. In this report, we describe the results obtained with 2′-*O*-methyl oligoribonucleotide derivatives of the previously selected aptamer (*15*). We demonstrated that a 2′-*O*-methyl RNA truncated version of the originally selected aptamer recognized the TAR RNA with properties similar to those of the parent RNA aptamer ($K_d \approx 10$ nM). This nuclease resistant oligomer selectively inhibited Tat-mediated transcription in a cell-free assay with an IC_{50} of ~400 nM in contrast to the unmodified molecule.

MATERIALS AND METHODS

Oligonucleotides. RNA molecules, including the biotinylated mini-TAR RNA, were synthesized as described previously (*15*). 2′-*O*-Methyl oligoribonucleotides (OMe) were synthesized on an Expedite 8908 synthesizer. All oligonucleotides were purified as described previously (*16*).

Oligonucleotide Stability in HeLa Cell Nuclear Extracts. $R06_{24}$ RNA (4 μM), OMe aptamer containing 2 nM ^{32}P 5′-end-labeled RNA, or OMe aptamer was incubated at 30 °C in transcription buffer {20 mM HEPES (pH 7.9) at 20 °C, 80 mM KCl, 3 mM $MgCl_2$, 10 μM $ZnSO_4$, 2 mM DTT, 10 mM creatine phosphate, 100 μg/mL creatine kinase, 1 μg of poly[d(I-C)], and 1 unit/μL RNasin} in the presence of 15 μL of HeLa cell nuclear extract in a final volume of 40 μL. The reaction was stopped by addition of 50 μL of a 150 mM sodium acetate solution containing 0.5% SDS, 10 mM EDTA, and 20 μg/mL tRNA. Reaction products were extracted with an equal volume of phenol and chloroform, followed by precipitation with 2 volumes of ethanol, and analyzed on 20% polyacrylamide, 7 M urea gels. The amount of full-length aptamer (percentage) was quantified on an Instant Imager apparatus (Hewlett-Packard).

UV Melting Experiments. Thermal denaturation of miniTAR with $R06_{24}$ RNA or OMe analogues was monitored at 260 nm on a Cary 1 spectrophotometer. Denaturation of the samples in 20 mM cacodylate buffer (pH 7.3) at 20 °C containing 140 mM potassium chloride, 20 mM sodium chloride, and 0.3 mM magnesium chloride was achieved by increasing the temperature at 0.4 °C/min from 5 to 90 °C. The melting temperature (T_m) was determined to be the maximum of the first derivative of the UV melting curves.

Surface Plasmon Resonance Kinetic Measurements. Binding kinetics experiments were performed at 23 °C on a BIAcore 2000 apparatus (Biacore AB, Uppsala, Sweden). Immobilization of streptavidin and biotinylated miniTAR RNA was achieved as described previously (*16*). All oligonucleotides were prepared in 20 mM HEPES buffer (pH 7.3) at 20 °C containing 20 mM sodium acetate, 140 mM potassium acetate, and 3 mM magnesium acetate (R buffer) and injected at a flow rate of 20 μL/min. The kinetic parameters were determined assuming a pseudo-first-order model as previously described (*16*).

Tat-Dependent Transcription Assays. Cell-free transcription assays were carried out as described previously (*19*, *20*). In vitro transcription reactions were performed in a final volume of 40 μL of transcription buffer supplemented with 50 μM ATP, CTP, and GTP, [α-^{32}P]UTP, 15 μL of HeLa cell nuclear extract, 10 nM HIV-1 LTR DNA template [plasmid p10SLT (*21*)], 200 ng of recombinant Tat protein, and increasing concentrations of aptamers. The samples were incubated at 30 °C for 20 min and the reactions stopped as described above for degradation experiments. Reaction products were analyzed on 6% polyacrylamide, 7 M urea gels and revealed by autoradiography. The autoradiographs were scanned. The amount of full-length transcripts was quantified from autoradiographs with the NIH Image 6.1 software. For HIV-1 Tat-independent in vitro transcription, the plasmid phRL-CMV (Promega) was linearized using *Nhe*I. Transcription reactions were carried out essentially as in Tat-dependent transcription with minor differences: the amount of DNA template was 200 ng, the KCl concentration was decreased to 50 mM, and the HIV Tat protein was not added to the reaction mixture.

RESULTS

$R06_{24}$-Derived Aptamer and MiniTAR RNA Target. RNA hairpins recognizing the HIV-1 TAR RNA were previously identified by in vitro selection in a random pool of sequences (*15*). These aptamers displayed an octameric 5′-GUCCCAGA-3′ consensus sequence in the loop and interacted with TAR primarily through loop−loop interactions (Figure 1A). The aptamer−TAR complex formed with the ligand of highest affinity, $R06_{24}$, was characterized, and the key structural determinants for stable interaction were analyzed (*16*). This included a six-nucleotide sequence complementary to the TAR loop, located in the apical loop of the hairpin, flanked by the selected G and A residues. In the study presented here, we investigated the properties of a 2′-*O*-methyl (OMe)-modified analogue of the $R06_{24}$ aptamer (Figure 1B) selected against the TAR motif of the BRU strain of HIV-1. The MAL variant of TAR which differs essentially by a U → C substitution in the loop (Figure 1C) was also used. An anti-TAR MAL aptamer was generated by introducing an A → G mutation. When unspecified, miniTAR, a truncated TAR which maintains biological responsiveness (*22*), and $R06_{24}$ refer to the BRU versions (*15*, *16*). In addition, two mutants of the aptamer loop, $R06_{24}$ 3A and CU (Figure 1C), were used as negative controls as these mutations were shown to decrease drastically the stability of the miniTAR−RNA aptamer kissing complex (*15*, *16*). These different aptamer variants and mutants were prepared both in the RNA and in the OMe series.

Stability and Kinetics of the MiniTAR−Aptamer Complexes. Complex formation was characterized first by thermal denaturation experiments as monitored by UV absorption spectroscopy (Figure 2). The experiments were performed in a buffer containing 0.3 mM Mg^{2+} instead of 3 mM Mg^{2+} in the selection buffer to avoid overlapping of the mono- and bimolecular transitions corresponding to the melting of

A

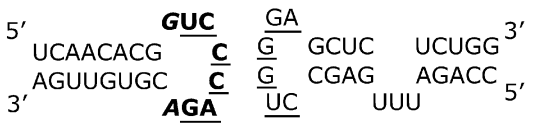

R06$_{24}$ aptamer **miniTAR RNA**

B

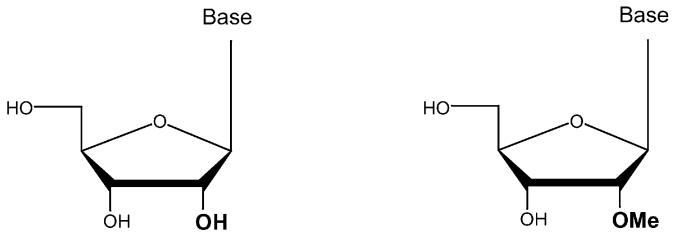

RNA **2′-*O*-Methyl (OMe)**

C

R06$_{24}$ aptamer		miniTAR RNA	
Name	**Sequence 5′ - 3′**	**Name**	**Sequence 3′ - 5′**
BRU	UCAACACG *G*UCCCAG*A* CGUGUUGA	**BRU**	GGUCUCUCG AGGGUC CGAGUUUAGACC
MAL	UCAACACG *G*UCCC**G**G*A* CGUGUUGA	**MAL**	GGUCUCUCG AGGG**C**C CGAG**CUG**GACC
CU	UCAACACG ***C***UCCCAG***U*** CGUGUUGA		
3A	UCAACACG *G*U**AAA**AG*A* CGUGUUGA		

FIGURE 1: R06$_{24}$ aptamers targeted to the HIV-1 miniTAR RNA. (A) Sequence and secondary structure of the R06$_{24}$ aptamer and miniTAR RNA. The octameric consensus sequence, including the loop flanking G and A nucleotides (bold italic) obtained from in vitro selection (*15*), is shown in bold. Underlined bases indicate complementarity between aptamer and TAR loops. (B) Schematic representation of the 2′-*O*-methyl (OMe) chemical modification compared to RNA. (C) Sequence of the mutated variants of the R06$_{24}$ aptamer (left) and miniTAR RNA (right). BRU and MAL refer to two HIV-1 strains differing in particular by apical loop sequences. The MAL aptamer was generated by introducing a compensatory mutation in the loop to restore complementarity with the TAR MAL loop (the mutated positions are shown in bold). The CU and 3A variants of the BRU aptamer were used as controls (see the text). The aptamer loop closing residues are in italics. The loop bases of the TAR element and of the aptamer susceptible to formation of Watson−Crick pairs are underlined.

the stem and of the loop−loop complex (*16*). R06$_{24}$ OMe exhibits a single cooperative transition (T_m = 77.6 ± 0.3 °C) independent of the oligonucleotide concentration compared to that of the unmodified R06$_{24}$ (T_m = 69.8 ± 0.3 °C, not shown). This result indicates that the OMe aptamer likely folds as a hairpin similar to the parent RNA molecule but with an increased stability. Three transitions are observed for the R06$_{24}$ OMe aptamer/miniTAR mixture. The first one at 29.0 ± 0.2 °C results from the melting of the bimolecular complex, and the second and third transitions at ∼60 and ∼78 °C reflect the melting of the miniTAR and aptamer hairpins, respectively. No complex formation was detected with the octamer corresponding to the consensus sequence (not shown), underlining the contribution of the stem to the stability of the complex.

We previously demonstrated the key role played by loop complementarity and the G and A residues flanking the aptamer loop for the stability of the miniTAR−aptamer RNA−RNA kissing complex (*16*). These key structural determinants are also crucial for stable interaction between the OMe aptamer and miniTAR. Indeed, if the three cytosines in the aptamer loop are substituted with three adenines (Figure 1), the stability of the complex is dramatically decreased from a T_m of 29 °C to a T_m of <10 °C (Table 1). A similar effect is observed when the G and A residues on each side of the aptamer loop are substituted with C and U, respectively (Figure 2 and Table 1). These values are similar to the ones obtained with the parent RNA molecule (Table 1). Complexes formed by the MAL sequences are clearly more stable than those with the BRU ones (Table 1). ΔT_m = +13 and +16.2 °C for the miniTAR RNA−RNA aptamer and miniTAR RNA−OMe complexes, respectively, in agreement with the GC pair content of the loop−loop helix (Figure 1C).

Surface plasmon resonance was used to follow in real time the interaction of the sensor chip-immobilized miniTAR RNA with the R06$_{24}$ OMe aptamer. Representative sensorgrams are presented in Figure 3. The kinetic parameters deduced from direct fitting of the curves obtained from three independent experiments in which R06$_{24}$ OMe was injected at five different concentrations, as indicated in Materials and Methods, have the following values: k_{on} = (9.0 ± 0.3) × 10^4 M^{-1} s^{-1} and k_{off} = (8.9 ± 0.6) × 10^{-4} s^{-1} for the association and dissociation reactions, respectively. These rates are slighly faster than those obtained for the RNA aptamer−miniTAR complex (*23*), but within experimental error, the equilibrium constant of the OMe aptamer−miniTAR complex remains unchanged compared to that of the RNA aptamer−miniTAR one with K_d values of 9.9 ± 1.0 and 6.9 ± 2.9 nM, respectively. The affinity of the CU

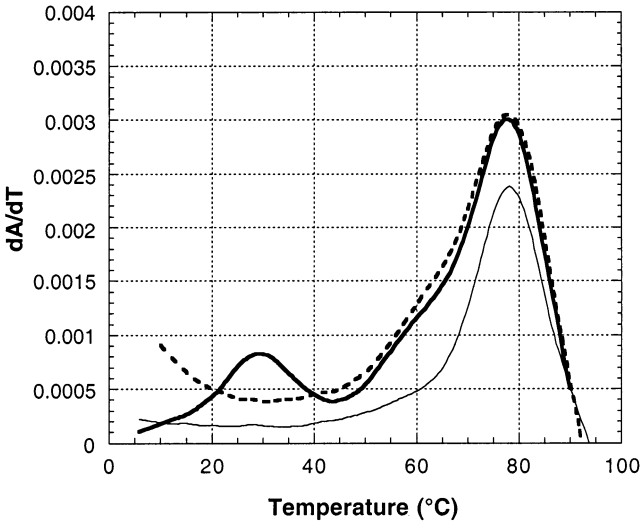

FIGURE 2: UV-monitored melting transition of aptamer−miniTAR complexes. First-derivative melting curve of $R06_{24}$ OMe alone (thin line) and complexed with miniTAR RNA (bold line and bold dotted line for BRU and CU aptamer variants, respectively). Experiments, repeated at least three times, were performed with each oligomer at 1 μM in 20 mM cacodylate buffer (pH 7.3) at 20 °C with 140 mM potassium chloride, 20 mM sodium chloride, and 0.3 mM magnesium chloride.

Table 1: Melting Temperatures of Aptamer−MiniTAR Complexes[a]

	T_m (°C)			T_m (°C)	
$R06_{24}$	TAR BRU	TAR MAL	$R06_{24}$	TAR BRU	TAR MAL
RNA			OMe		
BRU	30.3 ± 1.4	<10	BRU	29.0 ± 0.2	<10
CU	<10	ND	CU	<10	ND
3A	<10	ND	3A	<10	ND
MAL	11.5 ± 0.3	43.3 ± 0.7	MAL	16.3 ± 0.7	45.2 ± 0.5

[a] Thermal denaturations of miniTAR−aptamer complexes were performed for each oligomer (1 μM) in a buffer containing 0.3 mM Mg^{2+} (see Materials and Methods). T_ms are averages and standard deviations of at least three independent experiments.

mutant of the OMe aptamer for the miniTAR RNA was too low, and the binding constant could not be determined by SPR.

Inhibition of Tat-Dependent Transcription by the OMe-Modified Kissing Aptamer. We then investigated the ability of the RNA or OMe aptamer to selectively inhibit the Tat-mediated transcription of a DNA template in the presence of HeLa cell nuclear extracts. The DNA template contains the HIV-1 LTR (strain NL4-3) and a synthetic terminator sequence (τ) leading to the synthesis of two major RNA fragments that are 325 and 524 nucleotides long (Figure 4A). Addition of Tat protein resulted in a stimulation of the transcription as indicated by the increased intensity of bands corresponding to ^{32}P-labeled terminator (τ) and runoff transcription products (ρ) (Figure 4B, lanes a and l compared to lanes b and m). A clear dose-dependent inhibition of the transcription is observed with the chemically modified aptamer $R06_{24}$ OMe (Figure 4B, lanes c−e); 50% inhibition is reached at 388 ± 33 nM (Figure 4C). In contrast, the OMe aptamers with mutated loops 3A and CU which do not bind to the TAR RNA element (see above) do not inhibit RNA synthesis at concentrations up to 4 μM (Figure 4B,C), indicating that the inhibition induced with the wild-type aptamer is specific. The effect of $R06_{24}$ OMe was further

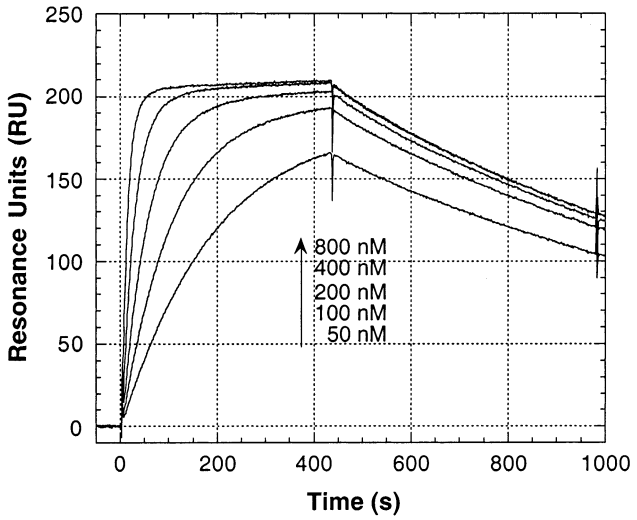

FIGURE 3: Sensorgrams of the $R06_{24}$ OMe−miniTAR RNA complex. Increasing concentrations of $R06_{24}$ OMe as indicated by the arrow were injected on a miniTAR-functionalized sensor chip. Three independent experiments were carried out in R buffer (3 mM Mg^{2+}) at 23 °C. Elementary rate constants, k_{on} and k_{off}, for bimolecular complex formation were deduced from direct fitting as described previously (*16*).

assessed by using a nonrelated DNA template containing a CMV promoter instead of the HIV-1 LTR (Figure 4D). No significant inhibition of transcription was observed in the presence of 1 or 4 μM wild-type $R06_{24}$ OMe or of one of its mutants, CU or 3A (Figure 4E).

The unmodified RNA aptamer exhibited a very weak inhibition of the HIV-1 template transcription with an IC_{50} of >4 μM (Figure 4B,C). This low inhibitory effect might be partly nonspecific, due to the trapping of TAR-binding proteins by RNA aptamers. The absence of an effect of the $R06_{24}$ RNA aptamer might be related to its low stability in cell extracts. Indeed, we monitored the stability of the RNA and OMe oligonucleotides by incubating them in HeLa cell nuclear extracts (Figure 5). While the RNA aptamer is rapidly degraded, the OMe aptamer is fully resistant to hydrolysis by the nucleases contained in the HeLa extract for up to 80 min.

DISCUSSION

Recently, we identified high-affinity ligands of the TAR element of HIV-1 through in vitro selection (*15*). These RNA aptamers do not disrupt the stem−loop secondary structure of TAR but rather interact with the folded RNA target with an affinity in the low nanomolar range. The aptamer of highest affinity, R06, forms with TAR a kissing complex which potentially comprises up to six intermolecular base pairs.

To obtain molecules of interest for use in a biological context, we derived nuclease resistant oligomers from a truncated version, $R06_{24}$, which retains the binding properties of the 98-nucleotide selected oligomer. In this respect, 2′-*O*-methyl modification is worth considering as a fully modified OMe oligonucleotide duplex adopts an A-type conformation characteristic of RNA−RNA helices which might be crucial for maintaining the loop−loop association between the modified aptamer and the TAR hairpins.

The OMe analogue of the $R06_{24}$ aptamer displays a highly cooperative melting transition with a ΔT_m relative to the

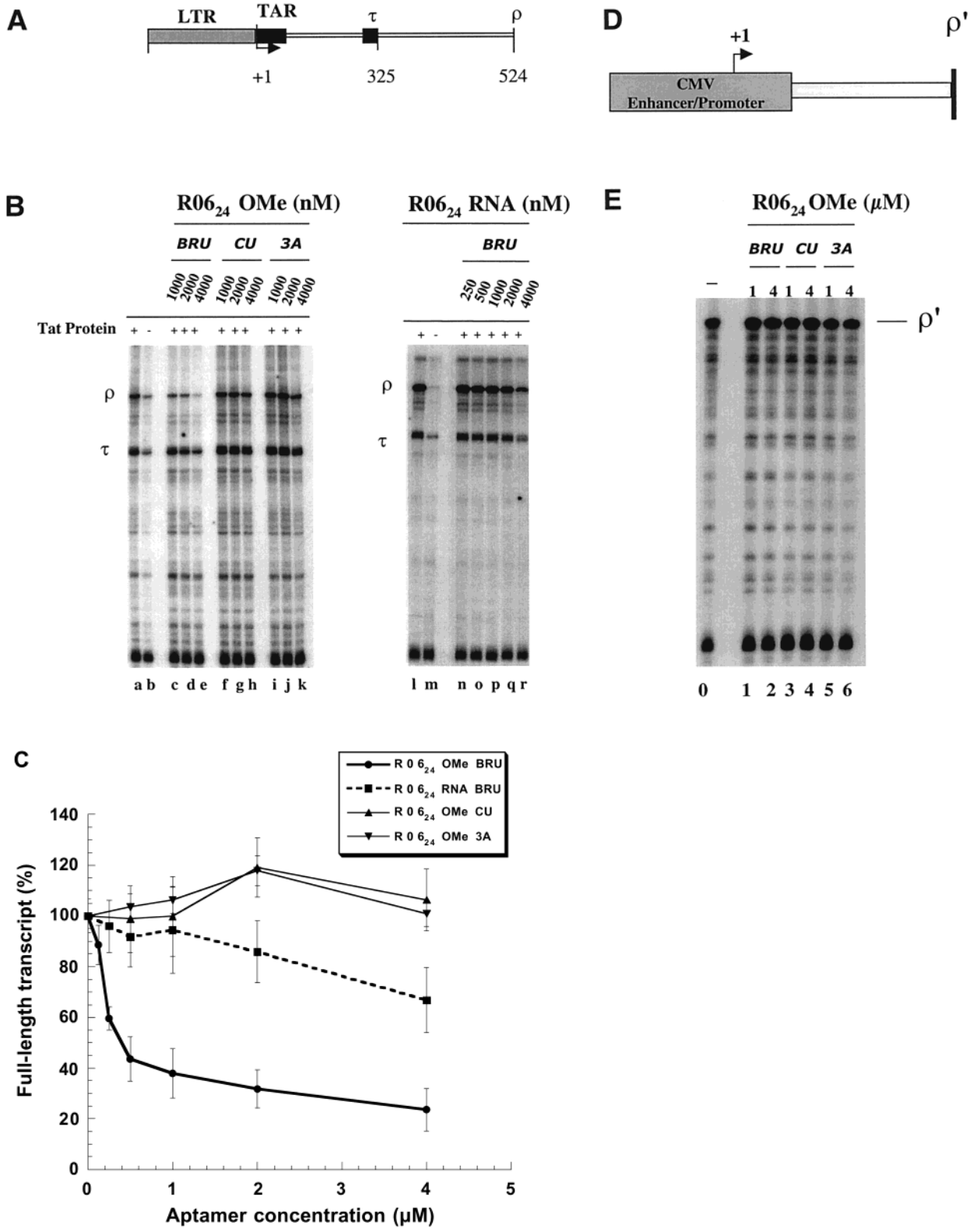

FIGURE 4: Inhibition of Tat-mediated in vitro transcription. (A) Schematic representation of the linearized DNA template containing the HIV-1 LTR promoter and an artificial terminator sequence (τ) used in this study. The transcription of this template generates two RNA products that are 325 (τ) and 524 (ρ) nucleotides long. (B) Autoradiographs of the transcription products analyzed on 6% polyacrylamide, 7 M urea gels. The DNA template (5 nM) was incubated in the presence of HeLa cell nuclear extract and in the presence (lanes a and l) or absence (lanes b and m) of 200 ng of recombinant Tat. R06$_{24}$ OMe and RNA wild-type (BRU) aptamers were added to in vitro transcription reaction mixtures at concentrations of up to 4 μM (lanes c−e and lanes n−p, respectively). The two mutated versions, R06$_{24}$ OMe CU and 3A, were also added to the transcription reaction mixtures at concentrations of up to 4 μM (lanes f−k). (C) Amount of full-length transcripts (ρ) as a function of aptamer concentration (values are the average of at least two experiments). **(**D) The nonrelated template containing CMV promoter is a phRL-CMV plasmid (Promega) linearized with *Nhe*I. The transcription of this resulting template leads to the synthesis of an RNA fragment that is 300 nucleotides long (ρ'). (E) Autoradiograph of transcription products analyzed on a 6% polyacrylamide, 7 M urea gel. In vitro transcription of the CMV DNA template in HeLa cell nuclear extract in the absence (lane 0) or the presence of R06$_{24}$ OMe BRU (lanes 1 and 2), CU (lanes 3 and 4), and 3A (lanes 5 and 6), at the concentration (micromolar) indicated at the top of the lanes.

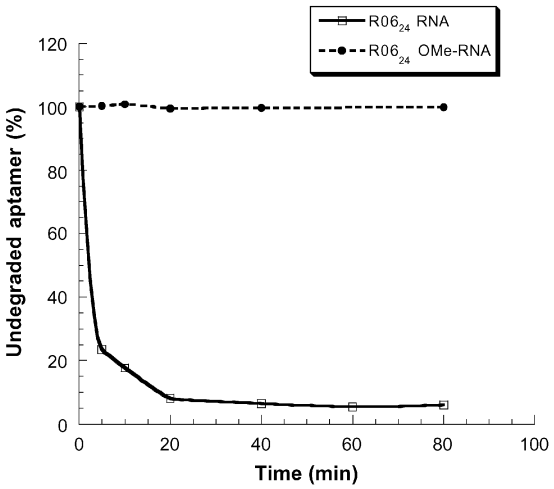

FIGURE 5: Aptamer stability in HeLa cell nuclear extract. Amount of full-length aptamer incubated in HeLa extracts at 30 °C as a function of time: R06$_{24}$ RNA (—) and R06$_{24}$ OMe (- - -).

RNA aptamer equal to +8 °C, corresponding to the melting of the eight-base pair stem (Figure 2). No direct correlation was observed between the intrinsic stability of the RNA aptamer stem and the complex formed with the TAR RNA target; despite its higher thermodynamic stability, the OMe aptamer gives rise to a complex characterized by a T_m value identical to that of the RNA aptamer. The equilibrium constant determined by SPR is fully consistent with this result; a K_d of ~10 nM was obtained for either complex. The increased stability ($\Delta T_m = +0.5$ °C per modification) of OMe−RNA versus RNA−RNA linear duplexes (*24*) is not observed in our case, underlining the noncanonical conformation of the loop−loop region. The complementary OMe sequence of the TAR loop has to be displayed in a hairpin context as the linear antisense is a poor ligand of the TAR element (not shown) as previously shown for RNA−RNA complexes (*16*). We still observed stable kissing complexes formed with an RNA aptamer truncated down to 14 nucleotides, i.e., showing a stem as short as three base pairs (F. Darfeuille et al., unpublished result). Stems are crucial for kissing complexes as they provide a continuous double-stranded stack from one end of the complex to the other through the loop−loop helix, but their stabilities do not drive the stability of the aptamer−TAR RNA complex.

Not unexpectedly, the complementarity between the TAR loop and the six central bases of the octameric consensus sequence of the aptamer is crucial for formation of a kissing complex. The presence of a single mismatch as in the case of complexes formed between BRU and MAL hairpins is detrimental to kissing interaction for OMe as well as for RNA aptamers. The selected G and A residues flanking the six-nucleotide sequence complementary to the TAR loop also play a key role in a 2′-*O*-methyl context. Substituting C for G and U for A in the R06$_{24}$ aptamer led to a very poor ligand as previously demonstrated for the parent RNA aptamer (*16*). Purine−purine pairs have been described in several different RNA motifs and have been shown to be crucial for either intermolecular or intramolecular RNA−RNA interaction. In particular, such noncanonical pairs are key elements of the α-sarcin (loop E) motif which has been described, for instance, in the IIId subdomain of the hepatitis C virus internal ribosome entry site (*25*, *26*) and for the dimerization of the HIV-1 RNA (*27*). In this latter case, two A residues closing a nine-membered loop are engaged in a sheared pair (*28*) that is crucial for formation of a kissing complex as shown by SELEX experiments (*29*). Therefore, the 2′-*O*-methyl derivative of R06$_{24}$ retains the binding characteristic of the parent RNA aptamer; the recognition of TAR by the aptamer hairpin is driven by a loop, complementary to the TAR one, flanked by G and A residues. Whether G and A form a noncanonical pair has not yet been established.

The high affinity of the anti-TAR RNA aptamer made it an efficient and selective inhibitor of TAR-mediated in vitro transcription. The efficacy of the OMe derivative compared to that of the unmodified RNA is likely related to its increased lifetime in the cell extracts. In contrast to the parent aptamer, no degradation of the nuclease resistant oligomer was detected in the time course of the transcription experiment. The transcription inhibition is dependent on the formation of an aptamer−TAR complex stable under the conditions of the experiment. No effect was observed with the OMe variant in which the critical G and A residues on each side of the aptamer loop were substituted with C and U, respectively, a substitution leading to an oligomer that is unable to bind TAR up to 5 μM. The binding constant ($K_d \approx 10$ nM) and the off rate constant ($k_{off} \approx 10^{-3}$ s^{-1}) of the R06$_{24}$ aptamer are in the range obtained for rationally designed antisense oligonucleotides (*19*, *20*). Indeed, R06$_{24}$ OMe induces a level of inhibition (50% at ~400 nM) analogous to that obtained with these antisense oligonucleotides. This selective inhibitory effect likely results from the competition with the protein(s) interacting with the upper part of the TAR element.

It should be pointed out that these elements provide kissing aptamers with an exquisite selectivity. Such aptamers will not only discriminate matched from mismatched loops, on the basis of sequence complementarity between the two interacting species (the hexameric motif). They will also recognize the appropriate target on the basis of its structure. A complementary sequence presented in a suboptimal context, for instance, inserted in a loop longer than the TAR one, will give rise to lower-stability complexes (F. Beaurain et al., unpublished results). In other words, aptamers targeted to an RNA motif constitute structure sensors even though the formation of the complex is primarily driven by Watson−Crick (sense−antisense) interactions, hence resulting in specificity that is increased compared to those of conventional antisense sequences.

Beyond our own previous work (*15*, *16*), several studies took advantage of secondary or tertiary interactions for improving the specificity and/or affinity of antisense sequences. Masked antisense RNA, in which most of the oligomer is sequestered within duplex elements prior to interacting with the target and which can unravel after contacting the sense sequence, was shown to exhibit an increased specificity compared to those of unfolded oligomers (*30*). A similar approach to overcoming the potassium requirement for triple helix formation with oligopurine sequences has also been described (*31*). However, in these cases, increased selectivity was achieved at the cost of reduced efficacy due to the energy to be paid for unfolding the antisense or triplex-forming sequence prior to completion of association. This is no longer a prerequisite for our aptamers or for the short oligomers targeted to the self-

splicing site in the rRNA precursor of *Pneumocystis carinii*. In this latter case, tertiary interactions stabilize by as much as 100000-fold the complex formed between the hexamer and the RNA splicing sequence. Indeed, complementary N3′ → P5′ phosphoramidate hexamers are suicide inhibitors of the cis-splicing reaction (*32*). Consequently, taking advantage of tertiary interactions for designing RNA ligands might constitute a strategy of general interest.

Natural antisense RNAs and retroviral RNA genomes provide examples of selective recognition of RNA motifs through loop−loop interactions. Kissing complexes have been shown to regulate the replication of the plasmids ColE1 (*33*) and R1 (*34*), to repress the translation of the *rpoS*-encoded σ^s subunit of *Escherichia coli* RNA polymerase (*35*), to trigger retroviral RNA dimerization (*36*, *37*), and to facilitate strand transfer during reverse transcription of the HIV-1 genome (*38*). Interactions between the apical loop and the internal loop have also been reported both for natural RNA species (*39*) and for selected partners (*14*). Besides these intermolecular interactions which selectively control key biological events, intramolecular loop−loop complexes have also been described; for instance, kissing interactions drive the rearrangement of a hairpin stem required for self-cleavage of the Varkud satellite ribozyme (*40*). Therefore, SELEX experiments carried out against RNA structures may help in understanding high-order organization of RNA.

ACKNOWLEDGMENT

We thank Justine Michel for the synthesis of the oligonucleotides. We also thank Jonathan Karn and Tony Lowe for the HeLa cell nuclear extract and the HIV-1 Tat protein.

REFERENCES

1. Sczakiel, G. (2000) *Front. Biosci. 5*, D194−D201.
2. Sohail, M., Akhtar, S., and Southern, E. M. (1999) *RNA 5*, 646−655.
3. Smith, L., Andersen, K. B., Hovgaard, L., and Jaroszewski, J. W. (2000) *Eur. J. Pharm. Sci. 11*, 191−198.
4. Lehmann, M. J., Patzel, V., and Sczakiel, G. (2000) *Nucleic Acids Res. 28*, 2597−2604.
5. Monia, B. P., Johnston, J. F., Sasmor, H., and Cummins, L. L. (1996) *J. Biol. Chem. 271*, 14533−14540.
6. Chen, T. Z., Lin, S. B., Wu, J. C., Choo, K. B., and Au, L. C. (1996) *J. Biochem. 119*, 252−255.
7. Peyman, A., Helsberg, M., Kretzschmar, G., Mag, M., Grabley, S., and Uhlmann, E. (1995) *Biol. Chem. Hoppe-Seyler 376*, 195−198.
8. Matveeva, O., Felden, B., Audlin, S., Gesteland, R. F., and Atkins, J. F. (1997) *Nucleic Acids Res. 25*, 5010−5016.
9. Allawi, H. T., Dong, F., Ip, H. S., Neri, B. P., and Lyamichev, V. I. (2001) *RNA 7*, 314−327.
10. Sohail, M., and Southern, E. M. (2001) *Methods Mol. Biol. 170*, 181−199.
11. Mir, K. U., and Southern, E. M. (1999) *Nat. Biotechnol. 17*, 788−792.
12. Amarzguioui, M., Brede, G., Babaie, E., Grotli, M., Sproat, B., and Prydz, H. (2000) *Nucleic Acids Res. 28*, 4113−4124.
13. Toulmé, J. J., Di Primo, C., and Moreau, S. (2001) *Prog. Nucleic Acid Res. Mol. Biol. 69*, 1−46.
14. Aldaz-Carroll, L., Tallet, B., Dausse, E., Yurchenko, L., and Toulmé, J. J. (2002) *Biochemistry 41*, 5883−5893.
15. Ducongé, F., and Toulmé, J. J. (1999) *RNA 5*, 1605−1614.
16. Ducongé, F., Di Primo, C., and Toulmé, J. J. (2000) *J. Biol. Chem. 275*, 21287−21294.
17. Osborne, S. E., Matsumura, I., and Ellington, A. D. (1997) *Curr. Opin. Chem. Biol. 1*, 5−9.
18. Kusser, W. (2000) *J. Biotechnol. 74*, 27−38.
19. Arzumanov, A., Walsh, A. P., Liu, X., Rajwanshi, V. K., Wengel, J., and Gait, M. J. (2001) *Nucleosides, Nucleotides Nucleic Acids 20*, 471−480.
20. Arzumanov, A., Walsh, A. P., Rajwanshi, V. K., Kumar, R., Wengel, J., and Gait, M. J. (2001) *Biochemistry 40*, 14645−14654.
21. Keen, N. J., Gait, M. J., and Karn, J. (1996) *Proc. Natl. Acad. Sci. U.S.A. 93*, 2505−2510.
22. Selby, M. J., Bain, E. S., Luciw, P. A., and Peterlin, B. M. (1989) *Genes Dev. 3*, 547−558.
23. Darfeuille, F., Cazenave, C., Gryaznov, S., Duconge, F., Di Primo, C., and Toulmé, J. J. (2001) *Nucleosides, Nucleotides Nucleic Acids 20*, 441−449.
24. Egli, M. (1996) *Angew. Chem., Int. Ed. 35*, 1894−1909.
25. Lukavsky, P. J., Otto, G. A., Lancaster, A. M., Sarnow, P., and Puglisi, J. D. (2000) *Nat. Struct. Biol. 7*, 1105−1110.
26. Klinck, R., Westhof, E., Walker, S., Afshar, M., Collier, A., and Aboul Ela, F. (2000) *RNA 6*, 1423−1431.
27. Lodmell, J. S., Ehresmann, C., Ehresmann, B., and Marquet, R. (2000) *RNA 6*, 1267−1276.
28. Jossinet, F., Paillart, J. C., Westhof, E., Hermann, T., Skripkin, E., Lodmell, J. S., Ehresmann, C., Ehresmann, B., and Marquet, R. (1999) *RNA 5*, 1222−1234.
29. Lodmell, J. S., Ehresmann, C., Ehresmann, B., and Marquet, R. (2001) *J. Mol. Biol. 311*, 475−490.
30. Stocks, M. R., and Rabbitts, T. H. (2000) *EMBO Rep. 1*, 59−64.
31. Svinarchuk, F., Cherny, D., Debin, A., Delain, E., and Malvy, C. (1996) *Nucleic Acids Res. 24*, 3858−3865.
32. Testa, S. M., Gryaznov, S. M., and Turner, D. H. (1999) *Proc. Natl. Acad. Sci. U.S.A. 96*, 2734−2739.
33. Tomizawa, J. I. (1984) *Cell 38*, 861−870.
34. Kolb, F. A., Malmgren, C., Westhof, E., Ehresmann, C., Ehresmann, B., Wagner, E. G., and Romby, P. (2000) *RNA 6*, 311−324.
35. Argaman, L., and Altuvia, S. (2000) *J. Mol. Biol. 300*, 1101−1112.
36. Paillart, J. C., Skripkin, E., Ehresmann, B., Ehresmann, C., and Marquet, R. (1996) *Proc. Natl. Acad. Sci. U.S.A. 93*, 5572−5577.
37. Kim, C. H., and Tinoco, I., Jr. (2000) *Proc. Natl. Acad. Sci. U.S.A. 97*, 9396−9401.
38. Berkhout, B., Vastenhouw, N. L., Klasens, B. I., and Huthoff, H. (2001) *RNA 7*, 1097−1114.
39. Ferrandon, D., Koch, I., Westhof, E., and Nusslein-Volhard, C. (1997) *EMBO J. 16*, 1751−1758.
40. Andersen, A. A., and Collins, R. A. (2001) *Proc. Natl. Acad. Sci. U.S.A. 98*, 7730−7735.

BI025974D